Published in 'Tribology International 39 (2006) 1361–1375'.

Studies of High Temperature Sliding Wear of Metallic Dissimilar Interfaces II: Incoloy MA956 versus Stellite 6

I.A. Inman*[a], S.R. Rose[b], P.K. Datta[b]

[a] *School of Engineering, Durham University, South Road, Durham, DH1 3LE, UK*
[b] *Advanced Materials Research Institute, Northumbria University, Newcastle upon Tyne, NE1 8ST, UK*

Abstract

The development of wear surfaces formed during limited debris retention sliding wear of Incoloy MA956 against Stellite 6 between room temperature and 750°C, and sliding speeds of 0.314 $m.s^{-1}$ and 0.905 $m.s^{-1}$ (7N applied load, 4,522 m sliding distance) were investigated. At 0.314 $m.s^{-1}$, mild oxidational wear was observed at all temperatures, due to oxidation of Stellite 6-sourced debris and transfer to the Incoloy MA956; this debris separated the Incoloy MA956 and Stellite 6 wear surfaces. Between room temperature and 450°C, the debris mainly took the form of loose particles with limited compaction, whilst between 510°C and 750°C the debris were compacted and sintered together to form a Co-Cr-based, wear protective 'glaze' layer. The behaviour was identical to that previously observed on sliding Nimonic 80A versus Stellite 6 at 0.314 $m.s^{-1}$.

At 0.905 $m.s^{-1}$, mild oxidational wear was only observed at room temperature and 270°C and dominated by Incoloy MA956-sourced debris. At 390°C and 450°C, the absence of oxide debris allowed 'metal-to-metal' contact and resulted in intermediate temperature severe wear; losses in the form of ejected metallic debris were almost entirely Incoloy MA956-sourced. This severe wear regime was also observed from 510°C up to 630°C, but increasingly restricted to the early stages of wear by development of a wear protective Incoloy MA956-sourced 'glaze' layer. This 'glaze' layer formed so rapidly at 690°C and 750°C, that severe wear was all but eliminated and wear levels were kept low.

The behaviour observed for Incoloy MA956 versus Stellite 6 at 0.905 $m.s^{-1}$ contrasts sharply with that previously observed for Nimonic 80A versus Stellite 6, in that the Incoloy MA956-sourced high Fe-Cr debris formed a protective oxide 'glaze', whilst the Nimonic 80A-sourced Ni and Cr oxides formed an abrasive oxide that at high sliding speeds assisted wear. The data indicates that the tendency of oxide to form a 'glaze' is readily influenced by the chemistry of the oxides generated.

Keywords: high temperature wear, dissimilar materials, oxide chemistry, 'glaze' layer, wear map

1. Introduction

The formation of 'glaze' layers during high temperature mild wear occurs when two metallic surfaces (or a metallic verses a suitable ceramic sliding surface) slide relative to one another under certain combinations of key tribological parameters, important amongst which are temperature, sliding speed and load. Extensive studies of the conditions required for 'glaze' formation have been conducted within AMRI [1-7] and elsewhere [8-29]; such studies indicate that where favourable conditions exist (especially at higher temperatures), a combination of elemental transfer, debris generation and oxidation of this debris can lead in combination with sintering reactions to the formation of wear protective, nano-crystalline 'glaze' layers [1, 2, 4].

---

* Corresponding author - *E-mail address:* i.a.inman@durham.ac.uk (I.A. Inman).

Studies by Lancaster [22], Welsh [23,24] So [25,26] and others [27-29] have shown that various combinations of load, sliding speed and temperature can have a dramatic effect on wear behaviour, particularly whether or not a protective 'glaze' can form. Additionally, several authors have constructed wear maps in an effort to present wear data in an easy to understand form, allowing prediction of the likely mode of wear under certain sliding conditions. Lim [30, 31] and Childs [32] designed wear maps based on load and sliding speed; however, other wear combinations can be used – for example, Kato and Hokkirigawa [33] developed an abrasive wear map, using as key parameters 'degree of penetration (of asperities)' and 'shear strength at the contact interface'. However, the majority of wear maps have been constructed using room temperature data – little work has been done on sliding at high ambient temperature or using dissimilar interfaces.

Within AMRI, study of the Nimonic 80A versus Stellite 6 wear pair [1,4,5] has indicated that sliding speed and temperature can together affect which surface undergoes greater wear and also the modes of wear observed in a dissimilar interface sliding system. For example, at low sliding speeds (0.314 $m.s^{-1}$ [1,4,5]), wear of the Stellite 6 surface dominated the process and the oxide debris generated from it was transferred to the surface of the Nimonic 80A. This Co-Cr oxide debris (in the form of a single co-oxide – Co_2CrO_4) separated the Nimonic 80A and Stellite 6 wear surfaces, in loose form at low temperature (room temperature to 450°C) and 'glaze' layers at high temperature (450°C to 750°C – these 'glaze' layers are nano-crystalline in nature [1-4]). A low (mild) wear regime was thus observed.

At higher sliding speeds (0.905 $m.s^{-1}$ [4,5], also 0.654 $m.s^{-1}$ [5]), generation of wear protective loose oxide debris (Co_2CrO_4) from the Stellite 6 was restricted to lower temperatures (room temperature and 270°C, also 390°C at 0.654 $m.s^{-1}$). Between 390°C (450°C at 0.654 $m.s^{-1}$) and 510°C, oxide debris was completely absent from the sliding interface and direct metal-to-metal contact favoured a severe wear regime and generation of primarily Nimonic 80A-sourced metallic debris. Oxide debris also generated from the Nimonic 80A surface reappeared at 570°C, but not in sufficient quantities to separate the metallic sliding surfaces and eliminate severe wear. Only on reaching 690°C and 750°C, was sufficient oxide produced to separate the wear surfaces; however, this mixture of separate Ni (NiO) and Cr oxides (Cr_2O_3) did not readily form 'glaze' and instead assisted the wear process by abrasion. The data collected allowed the development of a simple 'temperature versus sliding speed' wear map [5].

The readiness with which Co-Cr co-oxides formed a ‘glaze’ at lower sliding speeds, yet separate Ni and Cr oxides did not, was attributed to poorer sintering characteristics of the Ni and Cr oxides. Whilst at higher sliding speed, greater debris ejection and a more mobile environment would inhibit sintering, sliding speed alone could not account for the poor ‘glaze’ forming characteristics; Ni oxide generated in the absence of Cr oxide during the sliding of Nickel 200$^{\text{TM}}$ versus Stellite 6 at 0.905 m.s^{-1}, readily formed a ‘glaze’ at 750°C [1].

In the current study, the Fe-Cr Incoloy MA 956 (instead of Ni-Cr Nimonic 80A) is slid against Stellite 6 under identical conditions (room temperature to 750°C and sliding speeds of 0.314 m.s^{-1} and 0.905 m.s^{-1}). By effectively substituting Ni with Fe (both Nimonic 80A and Incoloy MA956 contain Cr), it is demonstrated that Cr in certain chemical compositions can also form part of a wear resistant ‘glaze’, even under conditions of high debris mobility and enhanced debris ejection at high sliding speed. The chemistry of the oxide is thus an important (and often neglected) consideration in ‘glaze’ formation. Finally, the data collected during the current study is combined with previous data collected by Rose at 0.654 m.s^{-1} [7], to produce a simple ‘temperature versus sliding speed’ wear map for the Incoloy MA956 versus Stellite 6 (counterface) wear pair (Fig. 14).

2. Experimental Details

The compositions of sample (Incoloy MA956) and counterface (Stellite 6) materials used for the experimental work are detailed in Table 1.

	Incoloy MA956 (sample)	Stellite 6 (counterface)
Ni	-	2.5 (maximum)
Cr	20	27
Ti	0.5	-
Al	4.5	-
Fe	74	2.5 (maximum)
Si	-	1
C	-	1
Co	-	60
W	-	5
Mn	0.05	1
Yt O	0.5	

Table 1: Nominal compositions of alloys (in wt.%)

All wear tests were carried out on a high temperature 'reciprocating-block-on-rotating-cylinder' wear rig in open air, as shown in Fig. 1 – this configuration tends not to encourage debris retention. Details of the high temperature wear machine used have been described previously [1,6,7] (the block forming the sample and the cylinder being the counterface). A variable speed electric motor rotated the shaft and connected counterface (Stellite 6) of diameter 50 mm and length 50 mm at various speeds. Cleaned samples of Incoloy MA956 polished to a 1 µm surface finish and of dimensions 5 mm x 5 mm x 45 mm were held against the counterface (polished to a 1200 grit surface finish and also cleaned) using a sample arm in reciprocating motion, with reciprocation at 3 cycles per minute and a constant stroke of 12 mm. The tests were carried out at sliding speeds of 0.314 $m.s^{-1}$ and 0.905 $m.s^{-1}$ (representing different speeds of rotation at the surface of the counterface), under a load of 7 N at various temperatures between room temperature and 750° C. The total sliding distance for all tests was 4,522 m.

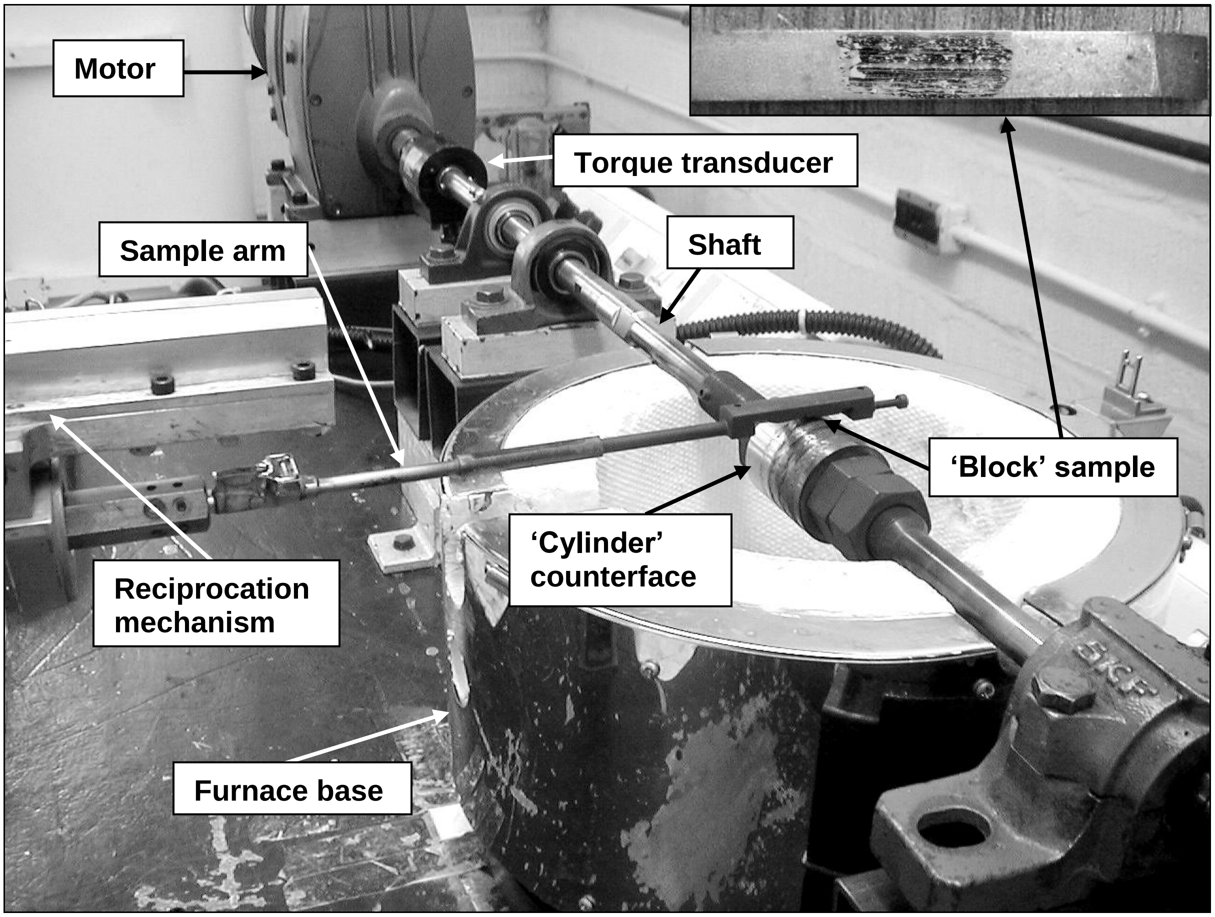

Fig. 1: Reciprocating high temperature block-on-cylinder wear rig, as used in the current experimental programme, plus a 'block' sample used during sliding experiments (shown example with 'glaze' layer formed by sliding at 0.905 $m.s^{-1}$ and 750°C)

A minimum of three sliding tests (one test per sample) were conducted for each combination of test conditions to ensure reproducibility of data; the weight of each sample was measured using a high accuracy Sartorious microbalance before and after sliding, from which a mean weight change value for each combination of sliding speed and temperature was calculated. The wear of the Stellite 6 counterface was briefly examined and not assessed quantitatively in this study – this is discussed in more detail elsewhere [3]. A Melbourne type TRP-50 torque transducer connected to the wear rig's rotating counterface shaft collected the coefficient of friction data.

The microstructures generated were characterised at the micro-scale level using scanning electron microscopy (SEM), energy dispersive analysis by X-ray (EDX) and X-ray diffraction analysis (XRD). Those samples slid at 750°C were additionally characterised using Atomic Force Microscopy (AFM).

Nano-indentation tests were additionally carried out on 'glaze' layers formed on Incoloy MA956 samples slid against Stellite 6 at 0.314 $m.s^{-1}$ / 510°C and 750°C, and 0.905 $m.s^{-1}$ / 510°C and 750°C, using a Hysitron nano-indenter with a 150 nm Berkovich three-sided pyramidal indenter. The test time in each case was ten seconds, with five second ramp up periods to and ramp down periods from maximum load. The dwell time at maximum load was zero. The maximum load used was 5,000 µN unless otherwise stated; this was the highest load possible without the indenter penetrating the 'glaze' layer.

Samples of Stellite 6 were also worn against a Stellite 6 counterface at 750°C (using the same methodology, and sample and counterface geometry as used with the Incoloy MA956 samples), and sliding speeds of 0.314 $m.s^{-1}$ and 0.905 $m.s^{-1}$. This was to verify the high sliding speed integrity of any Stellite 6-sourced (i.e. Co-Cr [1-7]) 'glaze' layers formed.

3. Results

3.1 Wear at 0.314 $m.s^{-1}$

Very low weight losses due to wear were observed during sliding of Incoloy MA956 (sample) versus Stellite 6 (counterface) at 0.314 $m.s^{-1}$ between room temperature and 450°C (Fig. 2). Over this temperature range, the wear surfaces of both the Incoloy MA 956 sample (Fig. 3) and Stellite 6 counterface (not shown) were covered in loose oxidised debris of size 300 nm to 1 µm (with a few debris outside this range) that became increasingly smeared at higher temperature. At 450°C, there was a little evidence of sintering and agglomeration of the debris and isolated areas of ‘glaze’-like material began to form. Evidence of metal-to-metal contact between room temperature and 450°C was extremely limited for the Incoloy MA956 / Stellite 6 system; monitoring of room temperature tests indicated that such contact was limited to the very early stages of wear, prior to oxide debris generation.

Weight change values remained very low between 510°C and 750°C (Fig. 2); however, with a tendency for slight weight gains. These gains coincided with formation of comprehensive ‘glaze’ layers on both sample (Fig. 3) and counterface (not shown), becoming more extensive and less porous as sliding temperature was increased. Under AFM (Fig. 4), a very fine ‘glaze’ grain structure was indicated at 750°C, with grain sizes as little as ~25 nm across; finer structures were possible; however, it was not possible to resolve these. Evidence of damage due to metal-to-metal contact between the Incoloy MA956 and Stellite 6 was less at ‘glaze’ forming temperatures and became progressively less evident on increasing the temperature towards 750°C. Loose oxide debris (again of size mostly between 300 nm and 1 µm) levels also decreased as the ‘glaze’ layers became more developed.

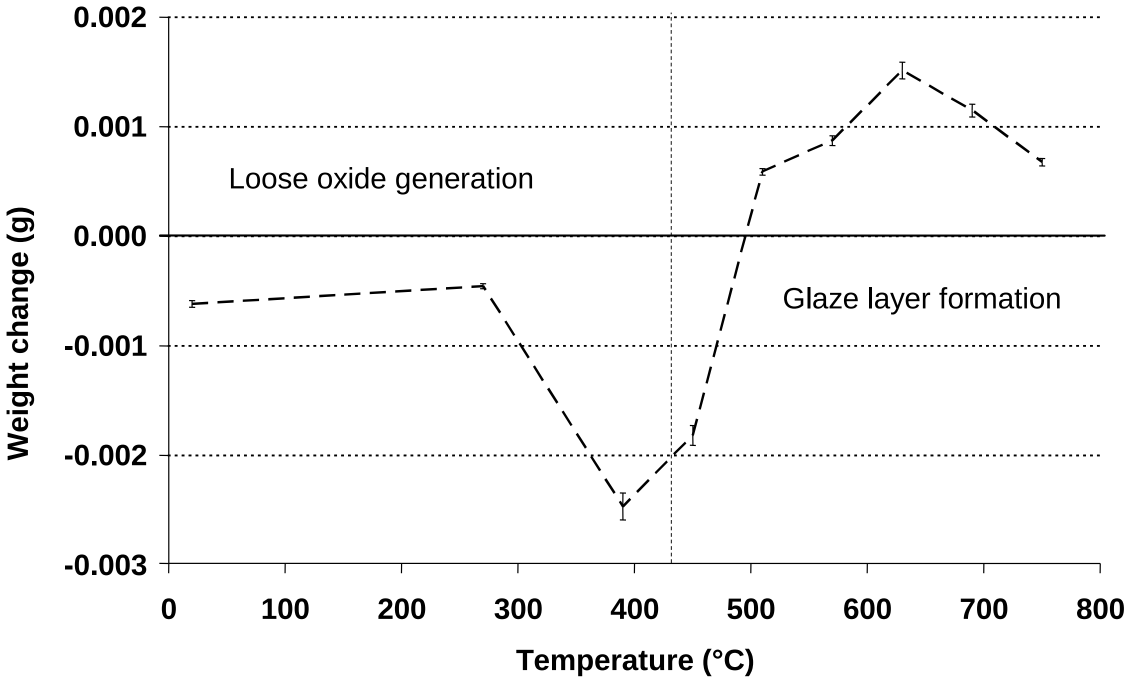

Fig. 2: Effect of temperature on weight change at 0.314 m.s^{-1}, with loose oxide generation below 450ºC and ‘glaze’ layer formation at 450ºC (limited) and above (comprehensive) – see Section 4 (discussion) for more information

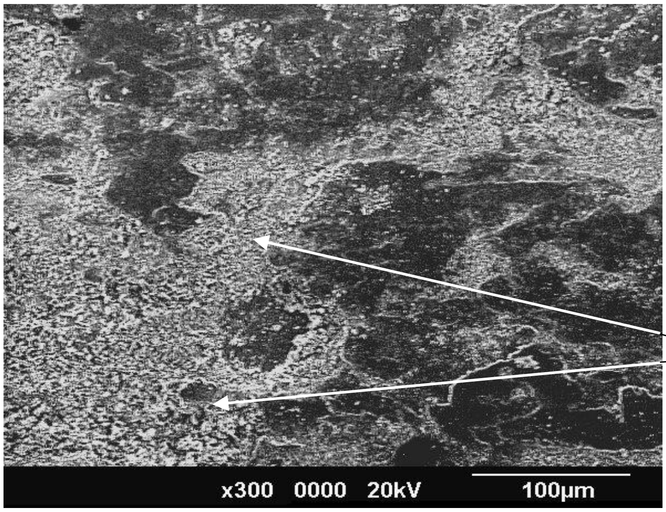	*A. Room temperature (shown), also typical of 270, 390 and 450°C* Loose oxide, plus some compacted oxide layers – isolated patches of 'glaze' at 450ºC only
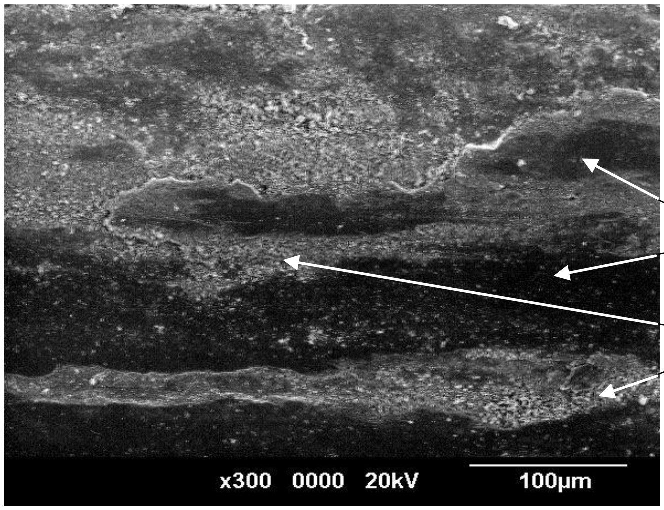	*B. 510°C* Areas of smooth 'glaze' layer formation Some accompanying loose debris.
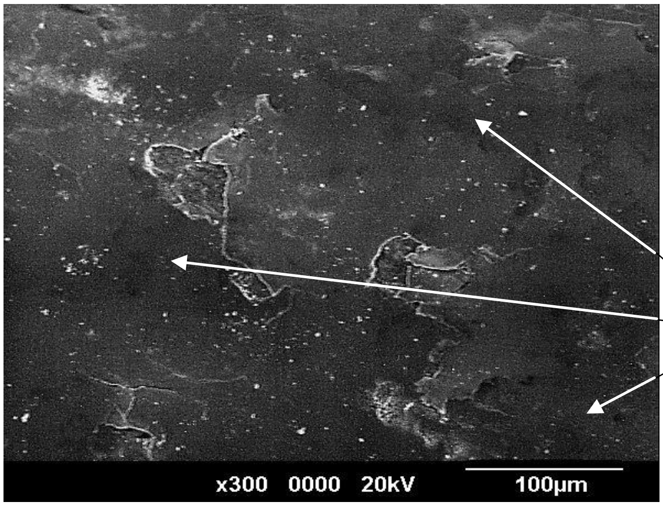	*C. 750°C (shown), also typical of 570, 630 and 690°C* Smooth 'glaze' layer formation with very little debris

Fig. 3: SEM micrographs of Incoloy MA956 wear surfaces after sliding at 0.314 m.s^{-1} against a Stellite 6 counterface at room temperature, 510 and 750°C

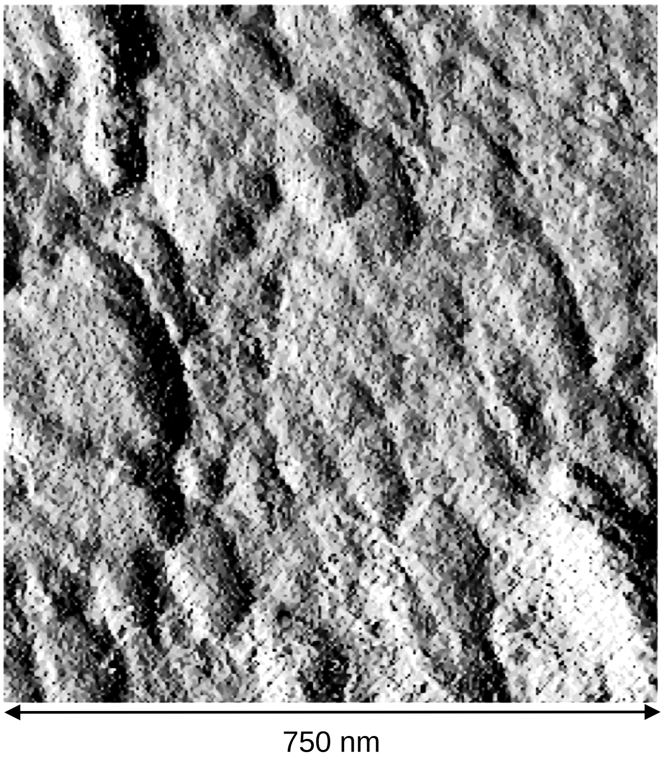

Fig. 4: Top-down AFM image of ‘glaze’ layer surface produced on Incoloy MA956 at 0.314 m.s^{-1} and 750°C

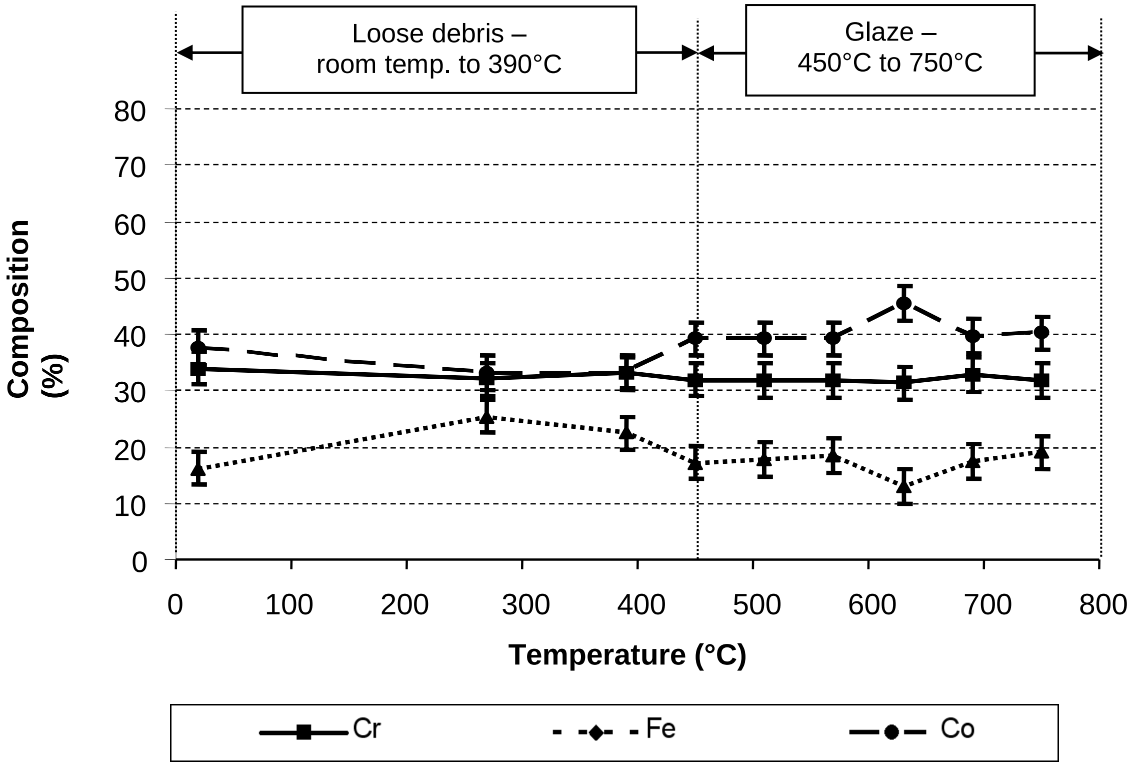

Fig. 5: Oxide debris and ‘glaze’ layer EDX data between room temperature and 750°C, 0.314 m.s^{-1}

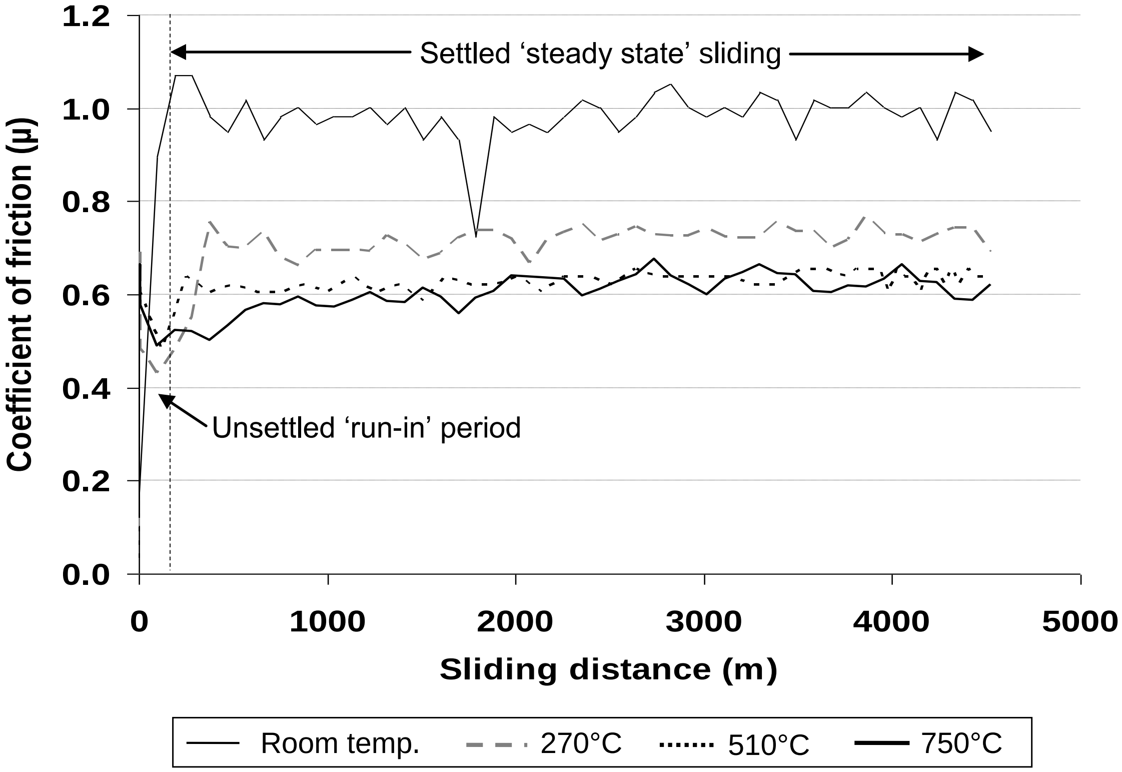

Fig. 6: Coefficient of friction versus temperature at 0.314 m.s^{-1}

The oxide debris and 'glaze' layers formed on the Incoloy MA956 wear scars showed a fairly consistent composition profile under EDX analysis (Fig. 5). Between room temperature and 390°C, high levels of Co (34% to 38%) and low levels of Fe (16% to 25%) indicated that most oxide debris was transferred from the Stellite 6, with only a limited Incoloy MA956 contribution. Between 450°C and 750°C, increased Co (~40%, occasionally ~45%) and decreased Fe (16 to 20%) indicated greater transfer from the Stellite 6. XRD analysis indicated the presence of one or both of the high Co phases $CoCr_2O_4$ and Co_3O_4 in the oxide debris, regardless of sliding temperature.

Measured coefficient of friction values (Fig. 6) showed two clear phases of behaviour; an initial unsettled 'run-in' period at the very beginning of sliding (variance ~20%), rapidly giving way to a more settled 'steady state' (variance ~12%), persisting for the remainder of each sliding test.

A downward trend in friction with temperature was apparent in both the data for the unsettled 'run-in' period and the 'steady state' period. This became less pronounced at higher temperatures, with no significant difference for either period between 510°C and 750°C data.

Peak values for the run-in data fell from 1.05 at room temperature, to 0.75 at 270°C, 0.64 at 510°C and 0.66 at 750°C; in each case a sharp rise from zero friction was observed at the beginning of testing. ‘Steady state’ values showed a steady decrease from between ~0.93 - 1.05 at room temperature, to between ~0.66 - 0.76 at 270°C, ~0.58 - 0.65 at 510°C and ~0.55 - 0.67 at 750°C.

Nano-hardness data indicated a high level of hardness at both 510°C and 750°C (Table 2). However, hardness levels at 510°C (mean 12.72 GPa) were significantly lower than at 750°C (mean 21.97 GPa). This difference can be attributed to the lower levels of sintering and greater porosity within the ‘glaze’ at 510°C, as can the high variability of the hardness values measured.

	$0.314\ m.s^{-1}$			$0.905\ m.s^{-1}$		
	Mean	Max.	Min.	Mean	Max.	Min.
510°C	12.72	16.54	6.90	17.51	23.82	12.28
750°C	21.97	28.39	17.51	15.45	22.65	6.74

Table 2: Mean ‘glaze’ layer nano-hardness data (all measurements in GPa)

3.2 Wear at $0.905\ m.s^{-1}$

On sliding Incoloy MA956 against a Stellite 6 counterface at $0.905\ m.s^{-1}$, losses due to wear were very low at room temperature and 270°C (Fig. 7). As at $0.314\ m.s^{-1}$, this low wear coincided with the presence of loose oxide debris of general size between 300 nm to 1 µm on both sample (Fig. 7) and counterface wear surfaces (not shown). However, there was more smearing of oxide particles at $0.905\ m.s^{-1}$ and metal-to-metal contact was slightly greater; some small metallic debris fragments were now present amongst the oxide debris. This smearing and damage due to metal-to-metal contact was more noticeable at 270°C

Oxide debris EDX analysis indicated greater levels of Fe (~56% at room temperature, ~30% at 270°C) and Cr (~36% at both temperatures), and reduced levels of Co (~8.5% at room temperature, ~30% at 270°C); XRD indicated Fe-rich $Cr_{1.3}Fe_{0.7}O_3$ in addition to $CoCr_2O_4$ and Co_3O_4. These data suggest a shift in primary debris source from Stellite 6 to Incoloy MA956.

At 390°C and 450°C, there was a large increase in Incoloy MA956 wear (Fig. 7). This was accompanied by a switch to a ‘severe wear’ mode, with both the Incoloy MA956 and Stellite 6 wear scars having a bright, torn metallic lustre (Fig. 8 shows the Incoloy MA956 wear scar at 450°C). Large amounts of metallic debris (5 to 20 µm in size) with no trace of oxide debris were now generated, with a composition typical of Incoloy MA956 (~62% Fe, ~28% Cr, 0.1%-0.4% Co) and XRD indicating a ferritic Fe-Cr phase. There was no evidence of material transfer from the Stellite 6.

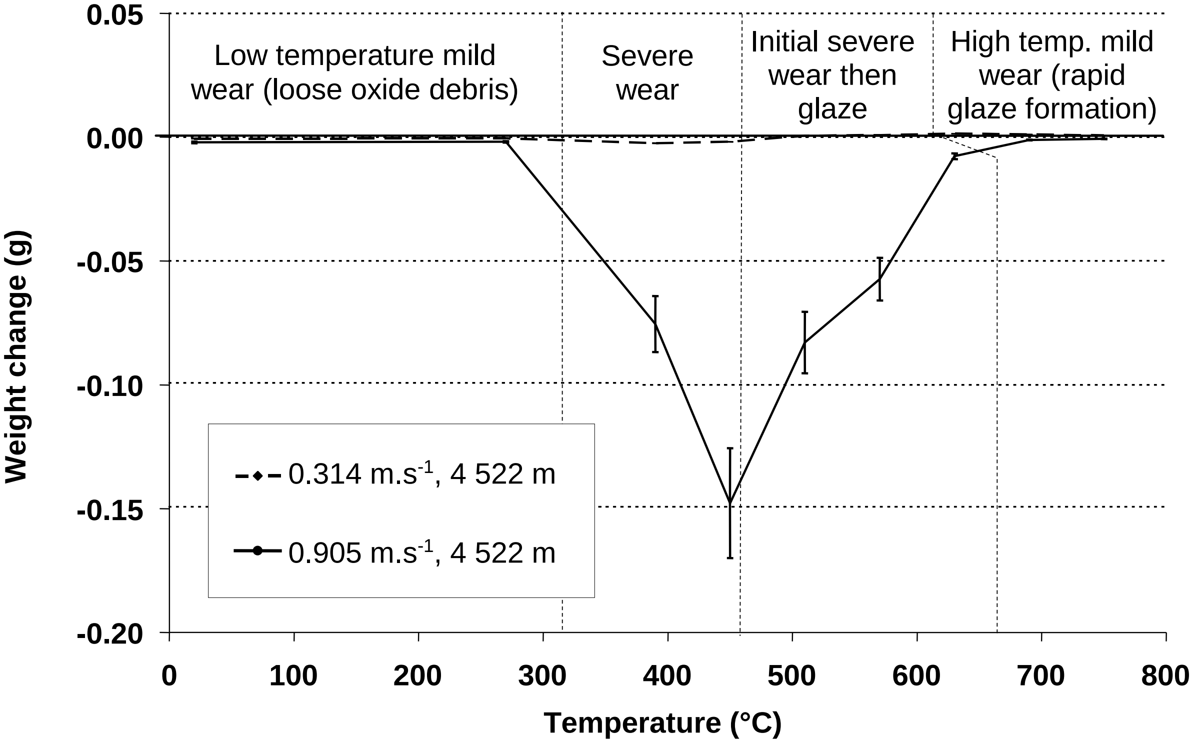

Fig. 7: Effect of temperature on Incoloy MA956 weight change and wear modes at 0.905 m.s^{-1} (0.314 m.s^{-1} data also shown)

Between 510°C and 750°C, a steady decrease in weight loss with increasing temperature was observed, reaching near negligible levels at 690°C and 750°C (Fig. 6); this decrease was accompanied by decreasing damage to both the Incoloy MA956 (Fig. 8) and Stellite 6 (not shown), and increasing levels of 'glaze' across the wear scar surfaces. The 'glaze' was patchy at 510°C (still absent from the counterface) and 570°C (now present on the counterface), but formed a comprehensive layer at 630°C and above. At 750°C, grain sizes were determined to be as little as ~25 nm in diameter using AFM (Fig. 9); finer structures were possible; however, as at 0.314 m.s^{-1}, resolution of such structures was not possible. The levels of metallic debris also decreased with greater sliding temperature, with increasing levels of oxide (of general size between 300 nm to 1 µm).

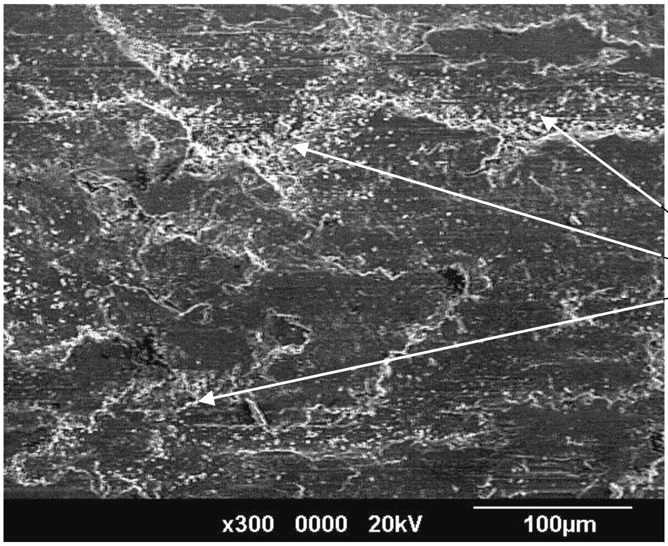

A. Room temperature (shown), also typical of 270°C

Loose oxide debris spread across wear surface (more smeared than at 0.314 m.s^{-1}), plus some compacted oxide formation and odd fragment of metallic debris (not shown)

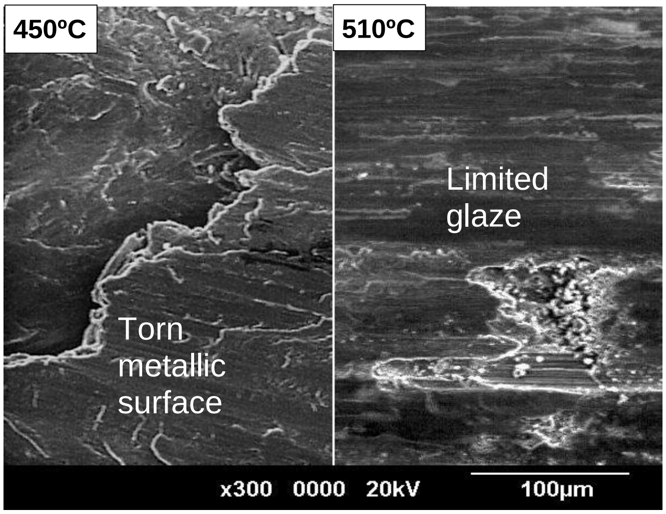

B. 450°C (left – also typical of 390°C) and 510°C (right – also typical of 570°C)

390ºC and 450ºC - torn, metallic surface typical of adhesive wear, no traces of any oxide debris

510ºC and 570ºC - very limited ‘glaze’ formation, more comprehensive at 570°C

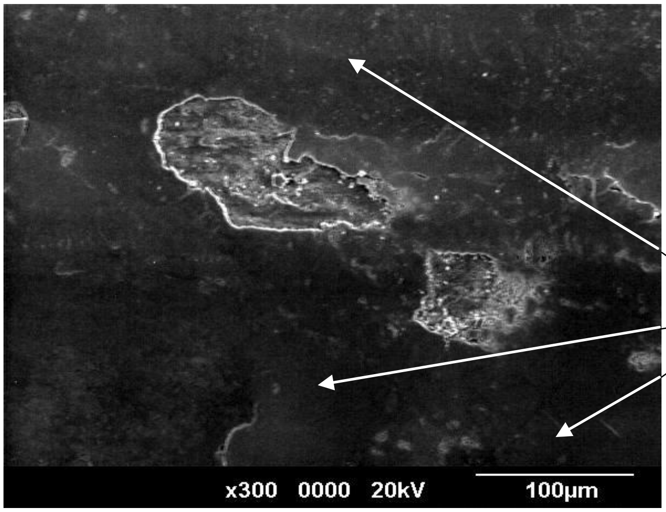

C. 750°C (shown), also typical of 630 and 690°C

Smooth ‘glaze’ layer formation with very little debris

Fig. 8: SEM micrographs of Incoloy MA956 wear surfaces after sliding at 0.905 m.s^{-1} against a Stellite 6 counterface at room temperature, 450, 510 and 750°C

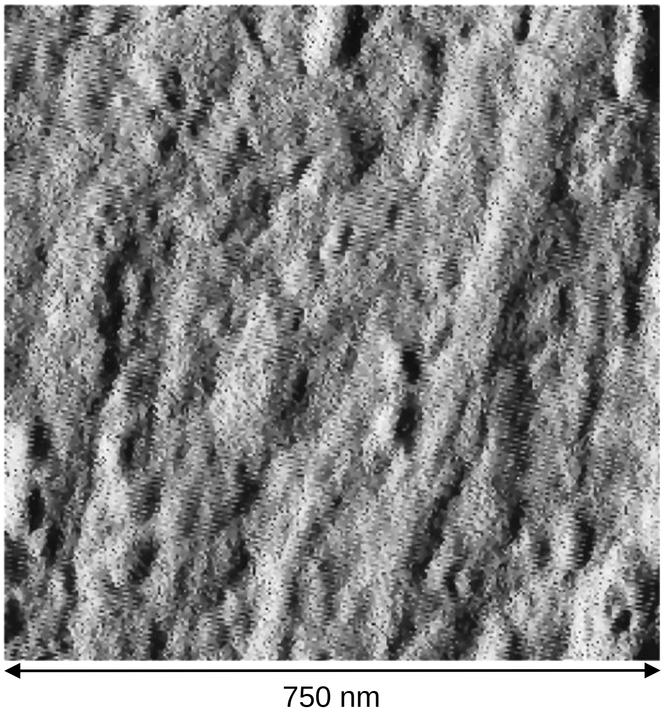

Fig. 9: Top-down AFM image of ‘glaze’ layer surface produced on Incoloy MA956 at 0.905 m.s^{-1} and 750°C

No compositional difference could be detected between the metallic and oxide debris by EDX, at temperatures of 510°C up to 630°C (typically ~67% Fe, ~26 to 28% Cr and only traces of Co – Fig. 10). In addition to the metallic debris’ ferritic Fe-Cr phase, XRD indicated both $Cr_{1.3}Fe_{0.7}O_3$ (however, EDX suggests a higher iron phase) and Co-containing $CoCr_2O_4$ phases in ‘glaze’ covered samples. The metallic debris and ‘glaze’-forming oxide were largely Incoloy MA956-sourced.

Only at 690°C and 750°C were there significant quantities of Stellite 6-sourced Co (up to ~15%) within the ‘glaze’ layers on the Incoloy MA956 and the now almost completely ‘oxide’ debris. However, Fe (~48%) and Cr (29 to 32%) continued to dominate (XRD indicating the presence of both $Cr_{1.3}Fe_{0.7}O_3$ – EDX again suggesting a higher iron phase - and $CoCr_2O_4$), showing that the Incoloy MA956 remained the main source of debris and ‘glaze’-forming material.

Other elements remained at negligible levels at 0.905 m.s^{-1} with the exception of Al, which between 450°C and 750°C was present within the ‘glaze’ to between 5% and 8%. Even higher levels of Al (up to ~24%) have been reported [1] using EDX mapping, suggesting preferential diffusion and oxidation of Al.

Coefficient of friction data at 0.905 m.s^{-1} (Fig. 11) were extremely variable and did not readily settle into a steady state. Any unsettled run-in period was thus difficult to distinguish from later data, though early increases from zero to on average ~0.52 at room temperature, ~0.63 at 270°C, ~1.16 at 510°C and ~0.71 at 750°C were noted.

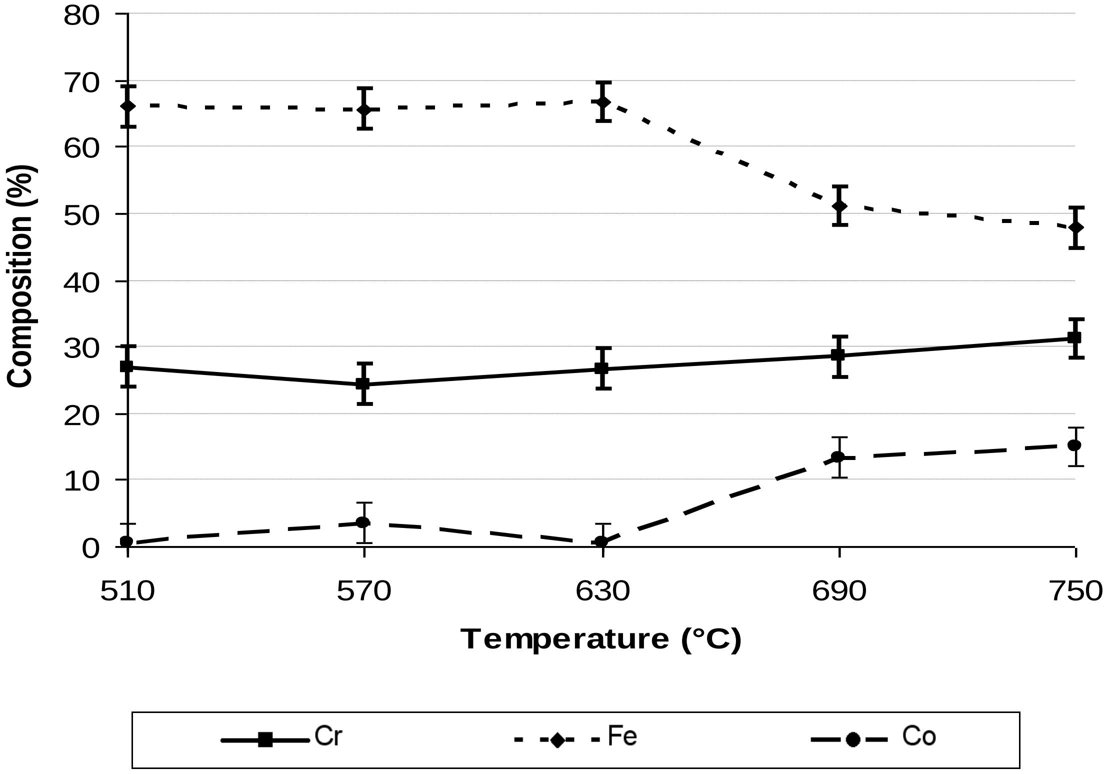

Fig. 10: Oxide 'glaze' layer EDX data between 510°C and 750°C, 0.905 m.s^{-1}

At 0.905 m.s^{-1}, steady state variations where identifiable of between ~0.34 and 0.52 at room temperature, ~0.41 and 0.65 at 270°C, ~0.36 and 0.68 at 510°C, and ~0.55 and 0.81 at 750°C were observed (variations were typically between ~20% and 33%). However, there were occasional large variations in friction, especially at room temperature and 270°C (for example, at room temperature, there was a rapid increase in friction from 0.37 after 2,449 m of sliding to 0.95 after 3,109 m).

Coefficient of friction values were lower at 0.905 m.s^{-1} than at 0.314 m.s^{-1}. However, greater vibration and reductions in contact time could mean actual coefficient of friction values at 0.905 m.s^{-1} may have been much higher. For this reason, it is difficult to draw any clear conclusions from the 0.905 m.s^{-1} data.

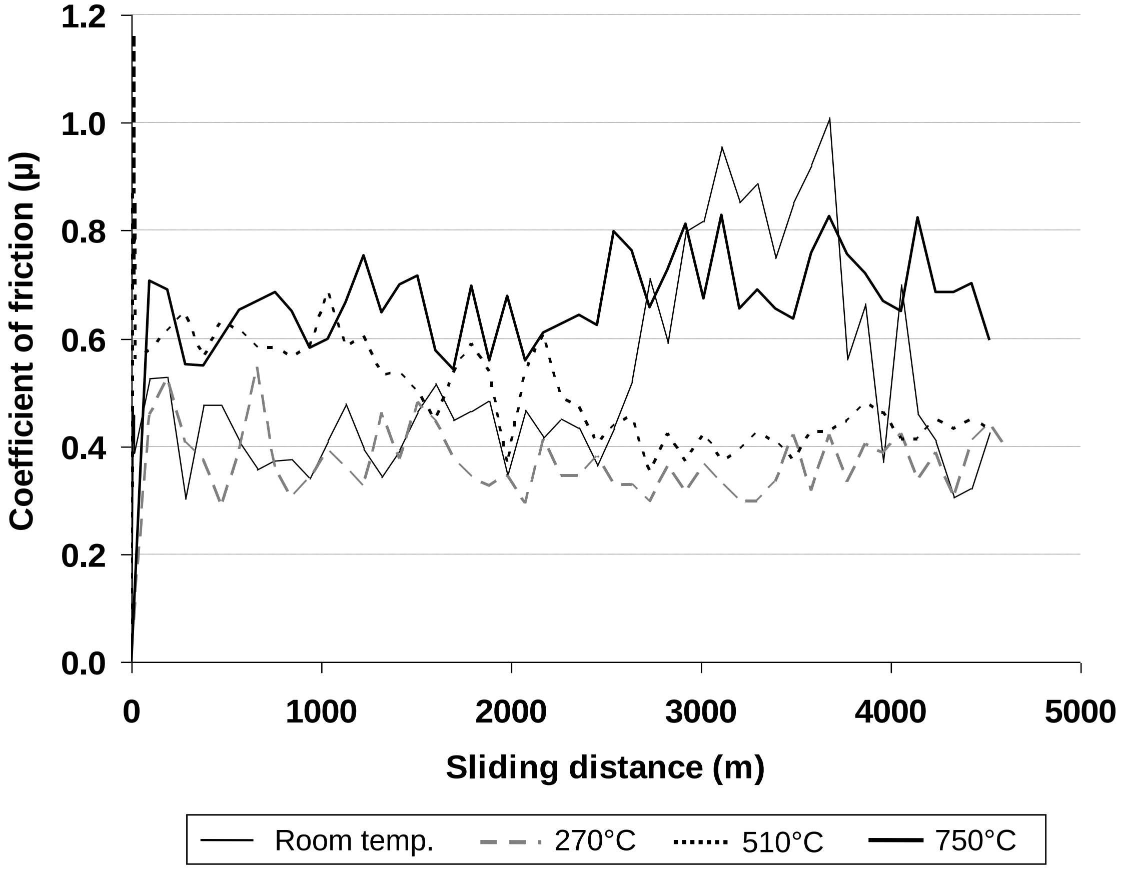

Fig. 11: Coefficient of friction versus temperature at 0.905 m.s^{-1}

High levels of hardness were indicated by nano-indentation data at both 510°C and 750°C (Table 2). There was no significant difference in hardness between the 'glaze' layers at 510°C (mean 17.15 GPa) and at 750°C (mean 15.45 GPa), despite the patchy nature of the 'glaze' at 510°C. Porosity within the 'glaze' layers again led to a wide range of values in the measurements taken, though the 510°C data seemed to be less variable.

3.3 Stellite 6 versus Stellite 6 at 750°C

Wear was extremely limited on sliding Stellite 6 versus Stellite 6 (0.0012 g at 0.314 m.s^{-1} and negligible at 0.905 m.s^{-1}), with 'glaze' layers forming readily on both sample and counterface surfaces regardless of sliding speed (Fig. 12) similar to those observed for Incoloy MA956 at 0.314 m.s^{-1} and 750°C. Damage during early sliding due to metallic contact was minimal, indicating extremely rapid formation of 'glaze' layers. 'Glaze' composition was consistent with that of Stellite 6 (~61% Co, ~25% Cr), with XRD indicating the oxide phase as either Co_3O_4 or $CoCr_2O_4$ at either speed; the high Co levels mean both phases were likely.

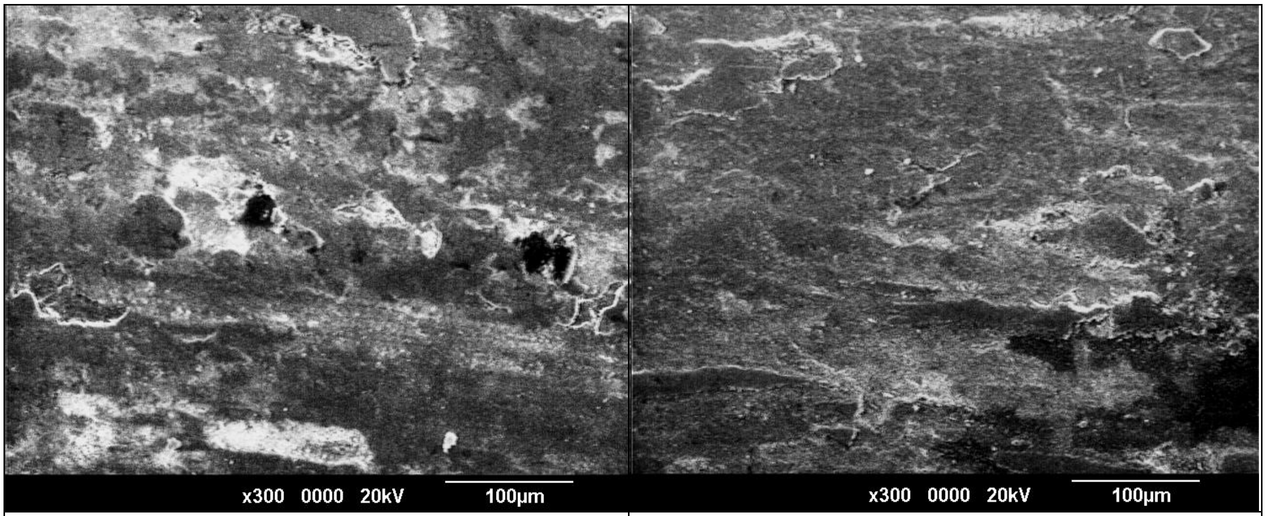

$0.314\ m.s^{-1}$ $0.905\ m.s^{-1}$

Fig. 12: ‘Glaze’ layers on sample sliding surfaces – Stellite 6 versus Stellite 6 at 0.314 $m.s^{-1}$ and 0.905 $m.s^{-1}$, 750°C

Only a brief run-in period could be identified from the coefficient of friction data at 0.314 $m.s^{-1}$ with values rising from zero to 0.7 (i.e. confirming ‘glaze’ formation was extremely rapid). A more settled steady state was quickly achieved, with values settling to between ~0.53 and 0.67 for the remainder of sliding. The data followed a similar pattern at 0.905 $m.s^{-1}$; however, with greater variation. Values during run-in rose from zero to 0.51, settling to between ~0.35 and 0.55 during steady state sliding. The higher variation and lower values at 0.905 $m.s^{-1}$ can again be attributed to greater vibration and reduced contact time.

4. Wear Map for Incoloy MA956 versus Stellite 6

In addition to the information presented within this paper, Rose previously presented data at 0.654 $m.s^{-1}$ (collected over a sliding distance of 9,418 m) [7] suggesting behaviour similar to that at 0.905 $m.s^{-1}$; however, wear transitions for the 0.654 $m.s^{-1}$ sliding speed were reported at temperatures of 60°C higher (these differences are discussed in Section 5.3). A revised set of weight change data is presented in Fig. 13 for sliding over 4,522 m (equivalent to that used for 0.314 $m.s^{-1}$ and 0.905 $m.s^{-1}$ in the current study), observations for which are identical to those at 9,418 m:

- A low loss, low temperature mild wear regime existed between room temperature and 390°C, with a mixed layer of discrete (mainly) Stellite 6-sourced Co-Cr oxide and also some Incoloy MA956-sourced Fe-Cr oxide particles separating the wear surfaces.

- A high loss ‘severe wear only’ regime due to direct metal-to-metal contact between sample and counterface existed only at 450°C. No oxide could be identified at this temperature.

- Substantial initial severe wear was observed on all samples slid between 510°C and 630°C. This severe wear phase became increasingly curtailed (and weight losses decreased) as the test temperature was raised, as primarily Incoloy MA956-sourced oxide debris deposition and ‘glaze’ formation became increasingly rapid.

- At 690°C and 750°C, there was very little evidence of severe wear before the onset of Incoloy MA956-sourced ‘glaze’ formation and weight losses at these temperatures were consequently very low. Rose reports that this oxide is Stellite 6-sourced [7]; however, fresh EDX indicates a composition consistent with Incoloy MA956 (~33% Fe, ~53% Cr, ~1.5% Co).

Using the information presented in this report, it is therefore possible to construct the following wear map for Incoloy MA956 when slid against Stellite 6 (Fig. 14), describing wear behaviour as a function of sliding speed and temperature. Each of the seven regions of wear identified in Fig. 14 is described in more detail in the following discussion.

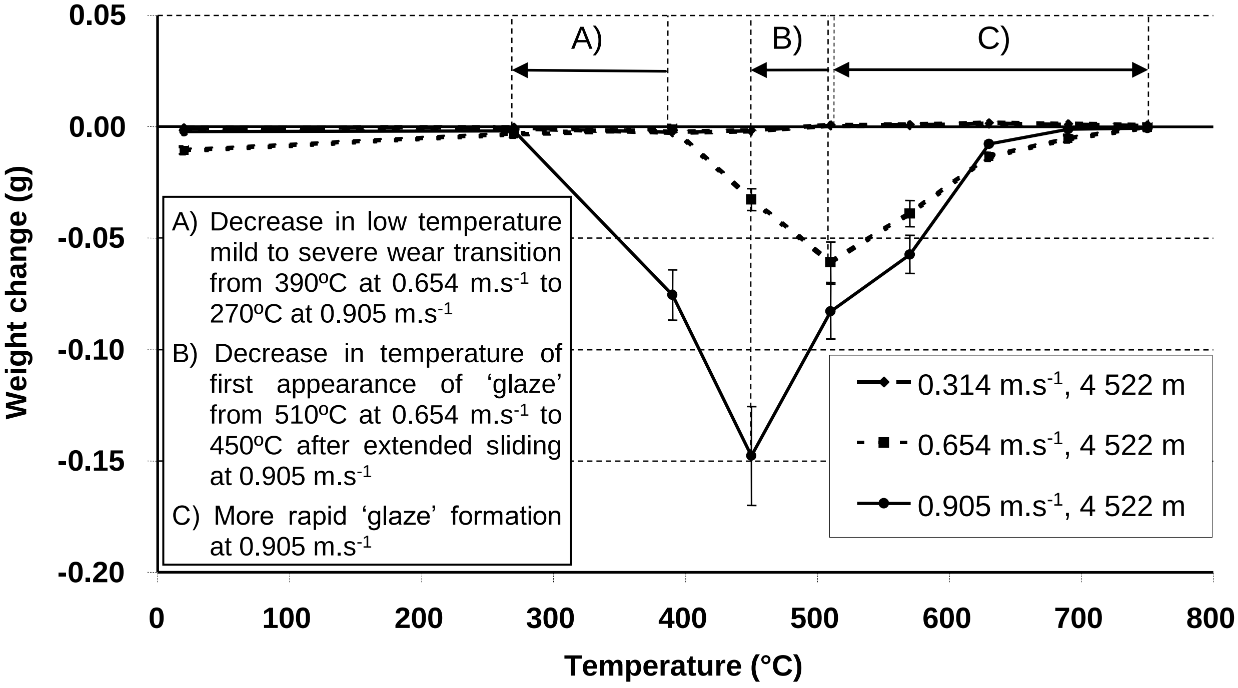

Fig. 13: Effect of temperature on Incoloy MA956 weight change and wear modes at 0.654 m.s^{-1} [7] (0.314 m.s^{-1} and 0.905 m.s^{-1} data also shown) – effect on transition temperatures on increasing sliding speed from 0.654 m.s^{-1} to 0.905 m.s^{-1} are indicated

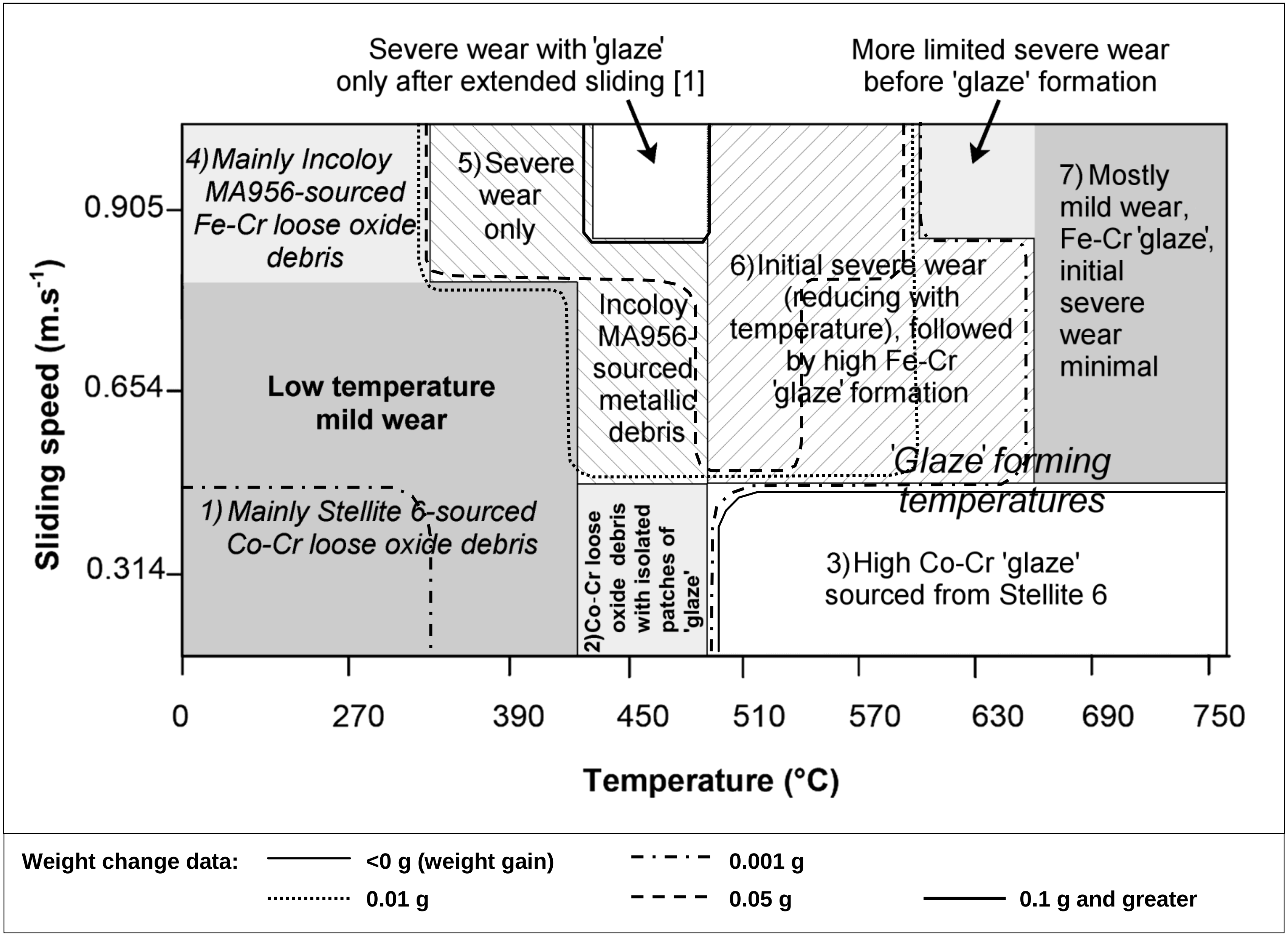

Fig. 14: Wear map for Incoloy MA956 slid against a Stellite 6 counterface (load 7N), with weight loss (contour) data superimposed

5. Discussion

5.1 0.314 m.s^{-1}

At 0.314 m.s^{-1}, the preferential wear of Stellite 6 at all temperatures strongly influenced the wear behaviour of the Incoloy MA956 / Stellite 6 (counterface) system. The wear process at 0.314 m.s^{-1} was thus dominated by debris generated from the Stellite 6 that rapidly transformed to oxide, transferred to the Incoloy MA956 surface and protected it from wear.

The primarily Stellite 6-sourced oxide debris (with some contribution from the Incoloy MA956) residing on the Incoloy MA956 surface (and Stellite 6 counterface surface), showed two types of behaviour depending on temperature. At less than 390°C (region 1, Fig. 14), the debris took the form of loose particles separating the wear surfaces (Fig. 3), hence reducing wear (Fig. 2). Particle agglomeration and consolidation increased at higher temperature with sintering first evident at 390°C and limited 'glaze' formation at 450°C (region 2, Fig. 14). Between 510ºC and 750ºC, the high hardness (Table 2), consolidated 'glaze' that formed (region 3, Fig 13, shown in Fig. 3) further reduced the wear of the whole system (Fig. 2); rapid oxide 'glaze' formation combined with extremely low levels of wear in fact led to an apparent slight weight gain over this temperature range. The formation of these 'glaze' layers was similar to that observed for the Nimonic 80A / Stellite 6 system at 0.314 m.s^{-1} [1-7]; the extremely fine grain size (measured at as little as ~25 nm using AFM – Fig. 4) indicates the likely formation of a nano-structured 'glaze' as described for Nimonic 80A / Stellite 6 [1-4]. It is worth noting that it appeared difficult to resolve very fine 'glaze'-surface detail using AFM and the actual grain structure may have been much finer; the use of STM in previous studies [1-4] was more successful.

Although the exact effect of each chemical element in the 'glaze' is uncertain, the presence of Co-based oxides clearly facilitates the rapid development of wear protective 'glaze' layers. The completely developed 'glaze' in the Incoloy MA956 / Stellite 6 system (between 510°C and 750°C) consisted of ~40% Co and ~32% Cr, again suggesting the presence of Co_3O_4 as well as $CoCr_2O_4$ (detected by XRD). However, the presence of moderately high levels of Fe (15-19% between 450°C and 750°C) indicates a significant Incoloy MA956 contribution to the 'glaze'. The role of the Fe at this time is unclear; however, the Fe did not noticeably alter the 'glaze' forming process for the Incoloy MA956 / Stellite 6 system, from that observed for

Nimonic 80A / Stellite 6 [1-7]. The formation of an Fe-Cr-based 'glaze' at 0.905 m.s^{-1} (510°C to 750°C) does not suggest a detrimental influence.

The greater wear of the Stellite 6 (in comparison to the Incoloy MA956) was originally thought to be caused by a delamination type of mechanism, possibly due to low fatigue crack growth resistance and K_{Ic} value of Stellite 6 [1]. Other data [34,35]; however, indicates a high K_{Ic} value for Stellite 6 compared to other alloys and why Stellite 6 undergoes greater wear at low sliding speed thus needs further investigation. One possibility already suggested for the Nimonic 80A / Stellite 6 wear pair [5] and also some steels by copper based material [36], is that oxide transferred from the harder member of the wear pair early during wear (i.e. Stellite 6) is embedded in the softer member's surface (i.e. the Incoloy MA956). A composite structure is created that enhances wear and oxide debris generation from the harder member as sliding continues.

Between room temperature and 390°C (region 1, Fig. 14), where the Stellite 6-sourced oxides did not form 'glaze', the abrasive nature of the loose oxides generated further promoted Stellite 6 wear. As for enhanced Stellite 6 wear at elevated temperatures (450°C and greater – regions 2 and 3, Fig. 14), the ΔG values in Table 3 indicate preferential oxidation of Co and Cr from the Stellite 6, which transferred to the Incoloy MA956 and rapidly formed into (and also later sustained) Co-based 'glaze'. The higher Fe levels at 270°C and 390°C temperatures (Fig. 3) may be attributable to the high tendency for Fe_3O_4 development (or Fe-Cr derivatives of) at intermediate temperatures (Table 3).

Stellite 6's hexagonal close-packed to face-centred cubic phase transformation is also a likely factor in 'glaze' debris generation – it is probable that frictional heating has raised the interfacial temperature sufficiently to promote this transformation. The formation of a face-centred cubic phase in Stellite 6 will lead to easier (easy dislocation slip) deformation, leading to greater material removal – this is discussed in more detail for the Nimonic 80A / Stellite 6 system [1-5].

The development of a sustained 'glaze' on the Incoloy MA956 (there was no evidence of disruption from carbides within the Stellite 6) is then followed by the back-transfer of the top part of the 'glaze' to the Stellite 6, facilitating the development of a Co-based 'glaze' layer on the Stellite 6 surface. There is thus a reduction in the overall wear of the system.

Oxide	**$\Delta G_{727^\circ C}$ (kJ.mol^{-1})**
$Co + ½O_2 \rightleftharpoons CoO$	-163.3
$3Co + 2O_2 \rightleftharpoons Co_3O_4$	-525.0
$2Cr + 1½O_2 \rightleftharpoons Cr_2O_3$	-861.6
$Fe + ½O_2 \rightleftharpoons FeO$ (dominant state above 500°C [14])	-197.2
$3Fe + 2O_2 \rightleftharpoons Fe_3O_4$ (favoured state between 200°C to 500°C)	-780.8
$2Fe + 1½O_2 \rightleftharpoons Fe_2O_3$ (favoured state below 200°C)	-556.8
$Ni + ½O_2 \rightleftharpoons NiO$	-150.7
$2Al + 1½O2 \rightleftharpoons Al_2O_3$	-1362.4
$W + O_2 \rightleftharpoons WO_2$	-405.7

Table 3: Free energies of formation for key oxides (Co, Cr and Ni) at 727°C under conditions of static oxidation [37]

5.2 Wear at 0.905 m.s^{-1}

Between room temperature and 270°C (region 4, Fig. 14), the presence of fine oxide debris particles (300 nm to 1 µm – Fig. 3), prevented direct metal-to-metal contact between the sample and the counterface. Adhesion between the Incoloy MA956 sample and Stellite 6 counterface and deformation of the sample were thus kept to a minimum and sample weight losses remained very low (Fig. 2). Higher Fe and lower Co levels in the oxides indicated that the Incoloy MA956 was now undergoing the greater wear at 0.905 m.s^{-1} and had become the primary source of debris. The continued presence of Co indicated that the Stellite 6 was also still undergoing some limited wear.

This situation was different from that observed for the Nimonic 80A / Stellite 6 (counterface) system where under similar conditions, the Stellite 6 remained the primary debris source at 0.905 m.s^{-1} [1,4,5].

This oxide debris retained on the Incoloy MA956 surface did not develop into a 'glaze'. A limited amount of deformation and spreading of this oxide was observed on the Incoloy MA956 surface, especially at 270°C. These deformed particles do not satisfy the conditions necessary for agglomeration and sintering; it is necessary for the particles to maintain their shape integrity, thus minimising their surface energy at the contact points between them. Only then can agglomeration and sintering occur, and 'glaze' layers develop. This loss of oxide debris shape integrity with increased temperature and poor debris retention allows for the observed increase in metal-to-metal contact at 270°C.

At 390°C and 450°C, any oxide debris generated could no longer prevent widespread metal-to-metal contact and a high loss, severe 'metal-to-metal' wear mechanism dominated (region 5, Fig. 14). Copious amounts of large, flat, metallic debris were generated predominantly from the Incoloy MA956, indicating wear by a delamination mechanism; however, this debris was not retained on the wear surfaces. The low residence and retention of debris meant that no 'glaze' formation could occur from any oxide produced on either surface. Thus high friction metal-to-metal wear continued to occur with enhanced wear of the softer Incoloy MA956, in a situation (Fig 5) resembling that for Nimonic 80A versus Stellite 6 under identical conditions [1,4,5]. Only after extended sliding (to 13,032 m) and only at 450°C, was sufficient oxide build-up to form 'glaze' layers reported [1].

At 510°C and above (region 6, Fig. 14), the degree of severe wear diminished with increasing temperature, due to increasingly rapid 'glaze' layer development across the Incoloy MA956 wear surface (Fig. 5). This reduction in severe wear was reflected by a reduction in the overall wear levels and at 630°C and above (region 7, Fig. 14), rapid 'glaze' formation prevented all but a brief period of severe wear and wear levels were extremely low. At such temperatures, the rate of oxide debris generation (from oxide forming on the Incoloy MA956 wear surface) was sufficient to exceed the rate of debris lost by ejection; this enhanced debris residency and allowed ‘glaze’ layers to form. The formation of this hard (Table 2), largely Fe-Cr-based ($Cr_{1.3}Fe_{0.7}O_3$ phase – however, the EDX data in Fig.10 suggests a higher Fe-containing phase), Incoloy MA956-sourced ‘glaze’ separated the wear surfaces, allowing further oxidational wear and layer formation; very limited amounts of Co-Cr oxide ($CoCr_2O_4$) were also incorporated from the Stellite 6.

The static free energies of formation favour the development of Co and Cr oxides from the Stellite 6 (Table 3). However, the increase in sliding speed from 0.314 $m.s^{-1}$ to 0.905 $m.s^{-1}$ has resulted in a shift toward the formation of other oxides including Fe from the Incoloy MA956. One anomaly with respect to these ΔG values is the high tendency for Fe-based oxide formation at intermediate temperatures (notably Fe_3O_4), which may in part explain the presence of more significant (but still low) levels of Co-containing oxides only at low and high (Fig. 10) sliding temperatures.

The difference in preferred Fe oxide phase (Fe_2O_3 up to 200°C, Fe_3O_4 between 200°C and 500°C and FeO above 500°C – Table 3) depending on temperature poses a problem for XRD data. Much XRD is conducted on material at room temperature once testing has finished. Whilst this gives a satisfactory result with oxides where there is no phase change on cooling (Co, Ni, etc.), room temperature XRD may not be appropriate where high Fe content oxides dominate. The Fe-Cr oxides generated during sliding of Incoloy MA956 against Stellite 6 at 0.905 $m.s^{-1}$ are a possible example and it cannot be guaranteed that the oxide phases observed at room temperature ($Cr_{1.3}Fe_{0.7}O_3$ and derivatives of) are the same as those generated at ‘glaze’-forming temperatures. It is suggested that conducting elevated temperature (i.e. hot stage) XRD on Fe-Cr oxide ‘glaze’ layers may be more useful.

The high levels of Al within the Fe-Cr ‘glaze’ layers can be attributed to preferential Al diffusion and oxidation from within the debris layers and possibly the Incoloy MA956 (ΔG for $2Al + 1\frac{1}{2}O_2 \rightleftharpoons Al_2O_3 = -1362.4$ – Table 3). Although the Al forms a small but significant part of the ‘glaze’ at 0.905 $m.s^{-1}$ / 750°C, the effect of Al on ‘glaze’ properties and development is at this time uncertain. However, aluminium oxide has elsewhere been observed to readily support ‘glaze’ formation [27].

The Incoloy MA956-sourced Fe-Cr ‘glaze’ formed at 0.905 $m.s^{-1}$ was observed to be more mechanically stable and less prone to break-up than the Stellite 6-sourced Co-Cr ‘glaze’ formed at 0.314 $m.s^{-1}$. The greater mechanical stability of this Incoloy MA956 sourced Fe-Cr ‘glaze’ is attributable to better and at times direct adherence of the oxide layers to the Incoloy MA956 wear surface; at 0.314 $m.s^{-1}$, the Co-Cr ‘glaze’ tended to overlie a powdery, poorly sintered layer of looser oxide debris.

The extremely fine grain structure (as low as ~25 nm) detected by AFM indicates the likely formation of a nano-structured ‘glaze’ as discussed elsewhere [1-4]. The morphology of this grain structure at first sight does not seem to have been affected by the sliding speed or the change in ‘glaze’ composition from largely Co-Cr at 0.314 $m.s^{-1}$ to Fe-Cr at 0.905 $m.s^{-1}$; however, this requires further investigation. However, as at 0.314 $m.s^{-1}$, there was some difficulty resolving very fine ‘glaze’-surface detail using AFM and a finer grain structure is possible.

As at 0.314 $m.s^{-1}$, the development of a sustained ‘glaze’ on the Incoloy MA956 (there was again no evidence of disruption from carbides within the Stellite 6) is then followed by the transfer of the top part of the ‘glaze’ to and the development of a ‘glaze’ layer on the Stellite 6. However, at 0.905 $m.s^{-1}$, the transferred ‘glaze’ is now predominantly Fe-Cr based. A reduction in the overall wear of the system still results, this becoming more substantial with increasing temperature as the ‘glaze’ layers develop more rapidly.

5.3 Differences between wear at 0.905 $m.s^{-1}$ and previous studies at 0.654 $m.s^{-1}$

The patterns of wear observed during current studies at 0.905 $m.s^{-1}$ were very similar to previous studies carried out by Rose at 0.654 $m.s^{-1}$ [7]. However, a number of differences were observed between the two sliding speeds.

Firstly, the difference in sliding speed was at room temperature and 270ºC, sufficient to affect the source of the loose oxide debris produced during low temperature mild wear. At 0.654 $m.s^{-1}$, the situation was very similar to that at 0.314 $m.s^{-1}$ with the mainly Co-Cr-based loose debris being primarily sourced from the Stellite 6 (region 1, Fig 13). At 0.905 $m.s^{-1}$, preferential wear of Incoloy MA956 resulted in the production of a mainly Fe-Cr-based oxide (region 4, Fig. 14).

The main differences in wear behaviour between the two sliding speeds; however, were the lower transition temperatures between wear regimes observed at 0.905 $m.s^{-1}$.

1. The lowering of transition temperature between low temperature mild wear and intermediate temperature severe wear, from 390°C at 0.654 $m.s^{-1}$ [7] (from region 1 to 5, Fig. 14) to 270°C at 0.905 $m.s^{-1}$ (from region 4 to 5, Fig. 14) occurs due to a combination of increased sliding speed and enhanced frictional heating. The loose oxide debris present during low temperature mild wear is less able to withstand the higher mechanical stresses and higher localised, frictionally induced temperatures at 0.905 $m.s^{-1}$. The shape integrity of the debris is thus only maintained sufficiently to prevent metallic interface contact up to 270°C at 0.905 $m.s^{-1}$; at 0.654 $m.s^{-1}$, shape integrity is maintained until 390°C. Above these temperatures, the greater loss of debris shape integrity (i.e. greater debris particle deformation) allows large scale metal-to-metal contact and severe wear to occur.

2. Enhanced frictional heating at 0.905 $m.s^{-1}$ also affects the transitions from intermediate temperature severe wear (region 5, Fig. 14) to severe wear followed by 'glaze' formation (region 6, Fig. 14), then high temperature mild wear with rapid 'glaze' formation (region 7, Fig. 14); this is due to faster production of oxide at 0.905 $m.s^{-1}$. 'Glaze' layers thus develop more quickly at 0.905 $m.s^{-1}$ and at lower test temperatures; 'glaze' is first observed at 450°C (after extended sliding [1] at 0.905 $m.s^{-1}$) compared to 510°C at 0.654 $m.s^{-1}$ [7]. However, wear at 0.905 $m.s^{-1}$ remains higher than at 0.654 $m.s^{-1}$ up to 630°C, due to greater material removal during pre-'glaze' formation severe wear. Wear at 0.905 $m.s^{-1}$ only fell below that for 0.654 $m.s^{-1}$ at 630°C and above, as increasingly rapid 'glaze' formation restricted this early severe wear (Fig. 13).

5.4 Differences between Incoloy MA956 / Stellite 6 and Nimonic 80A / Stellite 6

The modes of wear observed for both the Incoloy MA956 / Stellite 6 and Nimonic 80A / Stellite 6 systems [1,4,5] were very similar at 0.314 $m.s^{-1}$. The harder Stellite 6 underwent greater wear, the debris from which formed a loose oxide (room temperature to 450°C) or 'glaze' (510°C to 750°C) that facilitated low (mild) wear. The oxide was largely a Co-Cr oxide in both cases, with only a minimal contribution from the sample.

Equivalent wear regimes were also observed at 0.905 m.s^{-1} up to 450°C, with loose oxide generation and mild wear at room temperature and 270°C (though a shift from greater counterface to sample wear only happened for the Incoloy MA956 / Stellite 6 system), and severe wear (with high removal of sample material for both systems) at 390°C and 450°C.

Major differences were only observed at 0.905 m.s^{-1}, at temperatures of 510°C and above. Whereas for the Nimonic 80A / Stellite 6 system [1,4,5], the NiO and Cr_2O_3 oxides generated generally remained loose and assisted wear by abrasion (at best, a limited 'glaze' layer formed only on the Stellite 6), the Fe-Cr oxides generated in the Incoloy MA956 / Stellite 6 system formed 'glaze' layers progressively more rapidly (reducing early severe wear) as higher sliding temperatures were used (Fig. 15 - 750°C examples shown).

The change in oxide composition clearly indicates that high sliding speed alone is insufficient to prevent or inhibit oxide sintering needed to form 'glaze'. The Fe-Cr oxides show a much higher degree of sinterability, enabling debris to form 'glaze' even under conditions of high ejection and low residency encountered at 0.905 m.s^{-1}. The NiO and Cr_2O_3 oxides with poorer sinterability, cannot [1,4,5].

As previously discussed (by swapping sample and counterface for the Nimonic 80A / Stellite 6 system) [1,4,5], the transition from greater wear of counterface at 0.314 m.s^{-1} to greater wear of sample at 0.905 m.s^{-1} cannot be attributed to the 'block-on-cylinder' geometry of the system; the reasons for the transition are solely due to an increase in sliding speed. The transitions cannot be attributed to an inability of the Co-Cr 'glaze' layers generated at 0.314 m.s^{-1} to withstand the more aggressive conditions at 0.905 m.s^{-1}; by sliding Stellite 6 versus Stellite 6, it has been shown during this study that the Co-Cr 'glaze' layers are still highly wear protective at 0.905 m.s^{-1}. It is unclear at this time why this transition to greater sample wear was observed at 0.905 m.s^{-1} for both the Nimonic 80A / Stellite 6 [1,4,5] and the Incoloy MA956 / Stellite 6 systems; however, the reasons may be related to greater debris ejection, rather than transfer from Stellite 6, favouring wear of the sample.

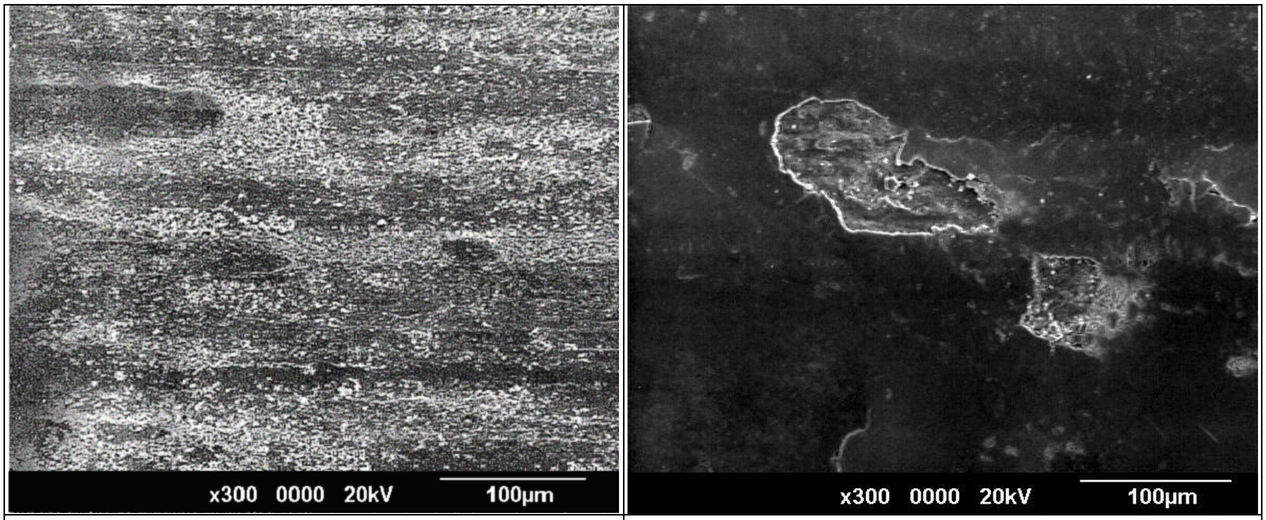

Nimonic 80A – loose Ni and Cr oxides

Incoloy MA956 – Fe-Cr oxide 'glaze' layer

Fig. 15: Oxides on sample sliding surfaces – Nimonic 80A [1,4,5] and also Incoloy MA956 versus Stellite 6 at 0.905 m.s^{-1} and 750°C

It is thus apparent from the data presented that the ability of an oxide to form 'glaze' depends not just upon sliding conditions, but also its chemical composition. For example, it has been seen that:

i) Co-Cr based oxides (i.e $CoCr_2O_4$) readily form wear protective 'glaze' layers at high temperature and as verified by the Stellite 6 versus Stellite 6 tests, at high sliding speed;

ii) Fe-Cr oxides can also form fairly robust wear protective layers under adverse sliding conditions; however,

iii) NiO and Cr_2O_3 oxides produced together from Nimonic 80A do not too readily sinter together to develop into 'glaze' [1,4,5], but NiO (produced from Nickel 200^{TM}) [1] will form a 'glaze' in the absence of Cr_2O_3.

6. Conclusions

The following behaviour was observed at 0.314 m.s^{-1}:

- A low temperature mild wear regime existed between room temperature and 450°C, with the wear surfaces separated by a layer of discrete mainly Stellite 6-sourced Co-Cr oxide particles.

- Mild wear persisted between 510°C and 750°C, with the mainly Co-Cr oxide sintering together to form comprehensive 'glaze' layers. The primary source of debris was once again the Stellite 6. Little evidence of initial severe wear could be found.

The following behaviour was observed at 0.905 $m.s^{-1}$:

- Low temperature mild wear existed only at room temperature and 270°C, with wear surfaces again separated by discrete mainly Fe-Cr oxide particles. The main source of debris was now the Incoloy MA956.
- 'Severe wear only' due to direct metal-to-metal contact was for 0.905 $m.s^{-1}$ observed at 390°C and 450°C ('glaze' develops at 450ºC only after extended sliding [1]).
- High losses due to severe wear became increasingly restricted on raising the temperature from 510°C to 750°C. The formation of wear protective 'glaze' layers from mainly Incoloy MA956-sourced Fe-Cr oxide occurred progressively earlier, until little early severe wear was observed at 690°C and 750°C; weight losses at these temperatures were consequently very low.

Additionally, the ability of a wear generated oxide to form 'glaze' layers depends not just upon the sliding conditions (i.e. sliding speed, temperature, etc.), but also on the chemical composition of the oxide. Where a 'glaze' does form, a nano-sized grain structure is likely.

References

[1] I.A. Inman, Ph.D. Thesis "Compacted Oxide Layer Formation under Conditions of Limited Debris Retention at the Wear Interface during High Temperature Sliding Wear of Superalloys", Northumbria University, UK (2003).

[2] I. A. Inman, S. Datta, H.L. Du, J.S. Burnell-Gray, S. Pierzgalski, Q. Luo, "Microscopy of 'glazed' layers formed during high temperature sliding wear at 750°C", Wear 254 (2003) 461-467.

[3] S. Datta, I. Inman, H.L. Du, Q. Luo "Microscopy of 'glazed' layers formed during high temperature wear, Invited Talk at the Institute of Materials", Tribology Meeting, London, November 2001.

[4] I.A. Inman, S. Datta, H.L. Du, J.S. Burnell-Gray, S. Pierzgalski and Q. Luo "Studies of High Temperature Sliding Wear of Metallic Dissimilar Interfaces", Trib. Int. 38 (2005) 812-823.

[5] I.A. Inman, S.R. Rose and P.K. Datta "Development of a simple 'temperature versus sliding speed' wear map for the sliding wear behaviour of dissimilar metallic interfaces (Nimonic 80A versus Stellite 6)" Wear (2005), *article in press*.

[6] P .D. Wood, Ph.D. Thesis "The Effect of the Counterface on the Wear Resistance of Certain Alloys at Room Temperature and 750°C", Northumbria University, UK (1997).

[7] S. R. Rose, Ph.D. Thesis "Studies of the High Temperature Tribological Behaviour of Some Superalloys", Northumbria University, UK (2000).

[8] F.H. Stott, D.S. Lin, G.C. Wood, "The structure and mechanism of formation of the "glaze" oxide layers produced on nickel-based alloys during wear at high temperatures", Corrosion Science 13 (1973) 449-469.

[9] M. Johnson, P. Moorhouse, J.R. Nicholls, DTI Industry Valve Project, 61-68 (1990).

[10] J-N. Aoh, J-C. Chen, "On the wear characteristics of cobalt-based hardfacing layer after thermal fatigue and oxidation", Wear 250-251 (2001) 611.

[11] Singh, J. and Alpas, A.T., "High-temperature Wear and Deformation Processes in Metal Matrix Composites," Metallurgical and Materials Transactions A, 27 (1996) 3135-3148

[12] F.H. Stott, J. Glascott, G.C. Wood, "Factors affecting the progressive development of wear-protective oxides on iron-base alloys during sliding at elevated temperatures", Wear 97 (1984) 93-106.

[13] M.G. Gee, N.M. Jennett, "High resolution characterisation of tribochemical films on alumina", Wear 193 (1995) 133-145.

[14] P.D. Wood, P.K. Datta, J.S. Burnell-Gray, N. Wood, "Investigation into the high temperature wear properties of alloys contacting against different counterfaces, Materials Science Forum", 251-254 (1997) 467-474.

[15] Wisbey, C.M. Ward-Close, Materials Science and Technology, "Wear resistant surfaces on high temperature titanium alloy and titanium aluminide by diffusion bonding", 13 (1997) 349-355.

[16] J. Jiang, F.H. Stott, M.M. Stack, "The effect of partial pressure of oxygen on the tribological behaviour of a nickel-based alloy, N80A, at elevated temperatures", Wear 203-204 (1997) 615-625.

[17] X.Y. Li, K.N. Tandon, "Microstructural characterization of mechanically mixed layer and wear debris in sliding wear of an Al alloy and an Al based composite", Wear 245 (2000) 148-161.

[18] J. Jiang, F. H. Stott, M. M. Stack, "A generic model for dry sliding wear of metals at elevated temperatures" Wear 256 (2004) 973-985.

[19] J. Jiang, F. H. Stott, M. M. Stack, "The role of triboparticulates in dry sliding wear" Trib. Int. 31-5 (1998) 245-256.

[20] J. Jiang, F. H. Stott, M. M. Stack, "Characterization of wear scar surfaces using combined three-dimensional topographic analysis and contact resistance measurements" Trib. Int. 30-7 (1997) 517-526.

[21] J. Jiang , F. H. Stott, M. M. Stack, "A mathematical model for sliding wear of metals at elevated temperatures" Wear 181-183 (1995) 20-31.

[22] J. Jiang, F. H. Stott, M. M. Stack, "Some frictional features associated with the sliding wear of the nickel-base alloy N80A at temperatures to 250 °C" Wear 176 (1994) 185-194.

[23] J.K. Lancaster "The Formation of Surface Films at the Transition Between Mild and Severe Metallic Wear", Proc. Royal Society London, A 273 (1962) 466-483

[24] N.C. Welsh "The Dry Wear of Steels 1, the General Pattern of Behaviour" Phil. Trans., 257A (1965) 31-50

[25] N.C. Welsh "The Dry Wear of Steels 2, Interpretation and Special Features" Phil. Trans., 257A (1965) 51-70

[26] H. So "Characteristics of Wear Results Tested by Pin-on-Disc at Moderate to High Speeds", Tribo. Int., Vol. 25, No. 5 (1996) 415-423

[27] H. So "Wear Behaviours of Laser-Clad Stellite Alloy 6", Wear 192 (1996) 78-84

[28] C. Subramanium "Wear of Al-12.3 Wt% Si Alloy Slid Against Various Counterface Materials" Scripta Metallurgica 25 (1991) 1369-1374

[29] P.J. Blau "Mechanisms for Traditional Friction and Wear Behaviour of Sliding Metals" Wear 72 (1981) 55-66

[30] S.C. Lim "Recent Development in Wear Maps", Tribo. Int., Vol. 31, Nos. 1-3 (1998) 87-97

[31] S.C. Lim "The relevance of wear-mechanism maps to mild-oxidational wear", Tribo. Int., Vol. 35, No. 11 (2002) 717-723

[32] T.H.C. Childs "The Sliding Wear Mechanisms of Metals, Mainly Steels", Tribo. Int., 13 (1980) 285-293

[33] K. Kato and K. Hokkirigawa "Abrasive Wear Diagram", Proc. Eurotrib '85, Vol. 4, Section 5.3, Elsevier, Amsterdam (1985) 1-5

[34] B.V. Cockeram "The Fracture Toughness and Toughening Mechanisms of Nickel-Base Wear Materials" Metallurgical and Materials Transactions A, 33A (2002) 33-57

[35] B.V. Cockeram "Some Observations of the Influence of d-Ferrite Content on the Hardness, Galling Resistance, and Fracture Toughness of Selected Commercially Available Alloys" Metallurgical and Materials Transactions A, 33A (2002) 3403-3419

[36] W Czupryk "Frictional Transfer of Iron in Oxidative Wear Conditions during Lubricated Sliding", Wear 237 (2000) 288-294

[37] E.A. Brandes and G.B. Brook "Smithells Metals Reference Book: Seventh Edition", Butterworth Heinemann (1992)

[38] H. So "Characteristics of Wear Results Tested by Pin on Disc at Moderate to High Speeds", Tribo. Int., Vol. 25, No. 5 (1996) 415-423

[39] K. Langgath, A. Kluge and H. Ryssel "Wear of Steels After Implantation of Oxygen Ions Or Oxidation at 670K", Wear 155 (1992) 343-351

[40] A. Iwabuchi, K. Hori, and H. Kudo "The Effect of Temperature, Preoxidation and Presliding on the Transition from Severe Wear to Mild Wear for S45C Carbon Steel and SUS 304 Stainless Steel" Proc. Int. Conf. Wear of Materials, New York (1987) 211-220

[41] F.H. Stott and D.R.G. Mitchell "The Influence of Coating on Wear at Elevated Temperatures" Surface Engineering, Volume 1 Fundamentals of Coatings, Ed. P.K. Datta and J.S. Gray (1993) 141-150

[42] P. Crook and C.C. Li "The Elevated Temperature Metal to Metal Wear Behaviour of Selected Hard Facing Alloys" Wear of Materials, ASME Publication 110254, (1983) 272-279

[43] T.F.J. Quinn "Review of Oxidational Wear. Part 1: The Origins of Oxidational Wear" Tribo. Int., 16 (1983) 257-270

Errata

Table 1 (Page 3): In the title, 'Nominal compositions of alloys (wt%)' reads incorrectly as 'Nominal compositions of alloys (at%)' in the online "Science Direct" version.